Bio-Inspired Hydrogels

DOI: 10.1002/anie.201200267

A Strong Bio-Inspired Layered PNIPAM–Clay Nanocomposite Hydrogel**

Jianfeng Wang, Ling Lin, Qunfeng Cheng, and Lei Jiang*

The demand for robust hydrogels in pharmaceutical, biomedical, and industrial applications has motivated intense research efforts in these wet polymeric materials.[1] Recent advances have resulted in different strategies for creating highly stretchable polymeric hydrogels, including sliding-ring gels (SR gels),[2] nanocomposite gels (NC gels),[3] double-network gels (DN gels),[4] macromolecular microsphere composite gels,[5] and tetra-poly(ethylene glycol) gels.[6] Among them, NC gels have attracted significant interest because of the simplicity of synthesis, high transparency, impressive mechanical properties, large reversible deformation, and excellent swelling and stimuli sensitivities.[7] The high mechanical properties of NC gels are desirable for practical application in many fields. However, it remains a great technical challenge to improve mechanical properties by enhancing the content of inorganic composition. Only a few percent of inorganic clay can be incorporated into NC gels (< 12 wt% at most), even though special mixing or modification of clay are adopted.[8] Further incorporation of clay leads to opacity and lower mechanical properties than the expected theoretical values resulting from the insufficiency of the nanoplatelet dispersion at high viscosity.

As natural inorganic–organic nanocomposites, nacre finds its way around this problem by developing a well-ordered brick-and-mortar microstructure and robust interface.[9] Although mostly made of mineral platelets, nacre possesses an excellent combination of elastic modulus, strength, and toughness [10] and it provides a prime microstructural design model for the development of new materials. Recently, the layered microstructure of nacre has been successfully mimicked and nacrelike hard structure materials with high mechanical performance were fabricated.[11] As for soft, wet inorganic–organic composites, NC gels can also benefit from duplication of the micro-/nanoscale structures of nacre. Herein, inspired by the ordered brick-and-mortar arrangement of inorganic and organic layers in nacre, we first demonstrate layered nanocomposite hydrogel (L-NC gel) films with a high clay content. The perfect micro-/nanoscale layered structure results in excellent mechanical properties higher than that of other reported NC hydrogels. We believe that it could offer innovative insights into the design of robust polymeric hydrogels for practical application.

In our experiment, we prepared layered poly(*N*-isopropylacrylamide)–nanoclay (i.e. PNIPAM-nanoclay) hydrogel films with a nacrelike structure (Scheme 1). In a first step, clay platelets with a diameter of 28.4 nm and a thickness of 1.11 nm, the NIPAM monomer and the initiator were assembled into a lamellar structure by vacuum filtration (Scheme 1 b).[12] Then, L-NC gels were synthesized easily by in situ radical polymerization of NIPAM initiated through UV light. After polymerization, none of the hydrogel films dissolved when kept in water for a long time or sonicated, implying that PNIPAM and clay successfully formed a kind of network structure. The structural model for L-NC gels is proposed, as shown in Scheme 1 c.

The L-NC gel films are highly transparent, almost irrespective of the clay content. Light transmittance measurements show about 50–95% of transparency across the visible spectrum of light (Figure S1 in the Supporting Information). The results indicate that an uniform dispersion of clay is achieved. The L-NC gel films did not distinctly change in transparency by altering the temperature across the lower critical solution temperature of PNIPAM. Probably the thermal molecular motion of the PNIPAM chains is restricted through interaction with a high content of clay platelets.[13]

The pure clay film was prepared by vacuum-filtration assembly, indicating a densely well-defined layered microstructure as shown in Figure S2 in the Supporting Information. The L-NC gel shows the overall structure with a strikingly alignment of the clay platelets, which are parallel to the film surface (Scheme 1 e and Figure S2 in the Supporting Information). The TEM image further shows well-defined and aligned self-assemblies with alternating hard clay and soft polymer layers (Scheme 1 f). The ordered microstructure was further elucidated by small angle X-ray power diffraction measurements (Figure S3 in the Supporting Information). Relative to the *d* spacing of 1.26 nm of pure clay,[14] for dried L-NC gels the *d* spacing increases to 2.2 nm, indicating that the PNIPAM layers are very thin. The structure is thus reminiscent of the brick-and-mortar structure of nacre,

[*] Dr. J. F. Wang, Prof. Q. F. Cheng, Prof. L. Jiang
Key Laboratory of Bio-inspired Smart Interfacial Science and Technology of Ministry of Education
School of Chemistry and Environment, BeiHang University
Beijing 100191 (P.R. China)
E-mail: cheng@buaa.edu.cn
Dr. L. Lin
Beijing National Laboratory for Molecular Sciences (BNLMS)
Key Laboratory of Organic Solids, Institute of Chemistry
Chinese Academy of Sciences
Beijing 100190 (P.R. China)

[**] This work was supported by the National Research Fund for Fundamental Key Projects (grant number 2010CB934700), the Research Fund for the Doctoral Program of Higher Education (grant numbers 20101102120044 and 20101102110035), the National Natural Science Foundation (grant numbers 51103004, 21003132, and 91127038), and the Scientific Research Foundation for the Returned Overseas Chinese Scholars, State Education Ministry, P.R. China.

Supporting information for this article is available on the WWW under http://dx.doi.org/10.1002/anie.201200267.

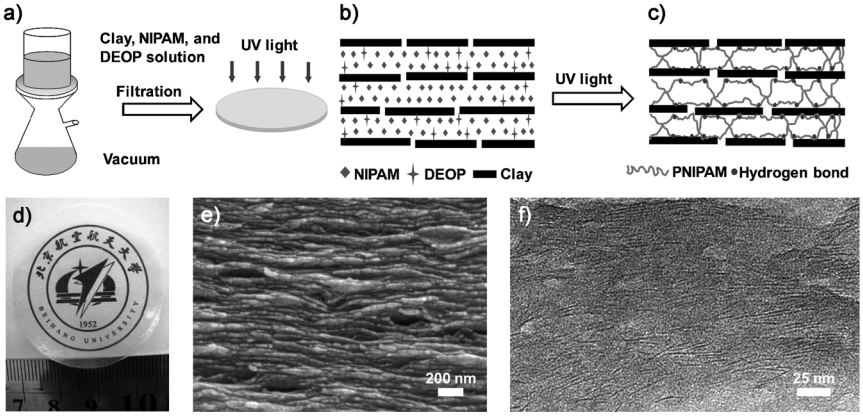

Scheme 1. a) Fabrication process of layered nanocomposite (L-NC) gel films. b) Assembled layered structure consisting of monomer, clay, and initiator. c) Proposed structural model for layered PNIPAM/clay hydrogels. The clay platelets act as multifunctional crosslinkers. The interaction between clay and PNIPAM is generally regarded as multiple hydrogen bonds. Simultaneously, PNIPAM chains adopt a coiled configuration. d) Digital photograph of a free-standing, transparent L-NC gel film. e) Cross-section morphology of a dried L-NC gel film, showing a strongly aligned layered arrangement. f) The TEM image further shows well-ordered stacks with alternating hard clay platelets and soft polymer layers.

although the layers have a smaller thickness and diameter than that in nacre. The orientation was probably assisted by directional flow induced by vacuum filtration.[15] The surface of the films is fairly flat with only some nanoscale roughness (Figure S4 in the Supporting Information). The mass ratio of clay and polymer in the resulting gels was identical and determined as approximately 67:33 by thermogravimetric analysis (TGA, Supporting Information).

Contrast random nanocomposite hydrogels (R-NC gels) show large elongation at break (around 880%; Figure 1a). Also, the clay content (ϕ_w) has an obvious effect on the tensile properties. The tensile strength and Young's modulus of R-NC gels increase with increasing clay content from 0.18 and 0.08 MPa at $\phi_w = 8.8$ wt% to 0.32 and 0.12 MPa at $\phi_w = 9.9$ wt%, respectively. At the same time, the large elongation at break is maintained. The results are consistent with the reported values for other photo-initiated PNIPAM/clay gels with similar clay content.[16] However, when the clay content further increases, the high viscosity leads to irregular aggregation of the clay. The transparency decreases and the mechanical property is distinctly deteriorated at $\phi_w = 10.9$ wt%.

L-NC gels show an unique tensile behavior which is different from R-NC gels. After linear elastic deformation, a well-defined yielding behavior appears, followed by hardening. The initial elastic modulus, yield stress, ultimate stress, and the slope in the hardening region significantly increase with increasing clay content from 11.3 to 23.2 wt%. Furthermore, the onset of the plastic deformation occurs at a smaller strain (Figure 1b). The tensile strength and elastic modulus at $\phi_w = 23.2$ wt% reach 1.6 and 43.2 MPa, respectively. The extensibility decreases slightly. Here, the L-NC gel with a clay content of 23.2% still shows a high elongation around 740%. The toughness calculated from the areas under the stress–strain curves reaches the maximum value (7.38 MJ m^{-3}) at $\phi_w = 23.2$ wt% (Figure 2a). The initial modulus of elasticity, ultimate tensile strength, and toughness for the L-NC gel at $\phi_w = 23.2$ wt% improve by 360, 5, and 6 times, respectively, relative to the R-NC gel at $\phi_w = 9.9$ wt%.

The excellent mechanical properties are attributed to the layered micro-/nanoscale structure and the unique polymer/clay network. In the network structure, clay platelets are uniformly dispersed, leading to a narrow distribution of distances between clay platelets.[3a] Furthermore, clay platelets acting as multifunctional crosslinkers are linked by a multiple flexible polymer chain. Hence, in the homogeneous polymer/clay network structure the load of clay platelets is spread over many chains. The noncovalent interaction between clay and PNIPAM is probably ascribed to hydrogen bonds between amide side groups (-CONH) on PNIPAM and the surface SiOH or Si–O groups of the clay.[17] However, as the PNIPA itself possess quite strong hydrogen-bonding interactions in the dried state, it is difficult to clearly observe hydrogen bonding to the clay in the dried L-NC gel (Figure S6 in the Supporting Information), which is consistent

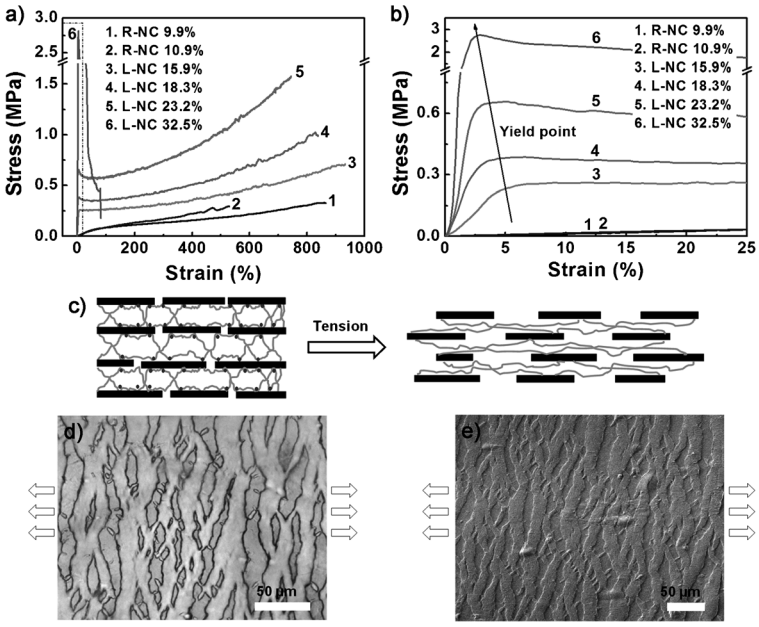

Figure 1. a,b) Tensile strength–strain curves for R-NC and L-NC gel films with different clay content. c) Structure changes of L-NC gels after tensile testing. The clay platelets slide on one another, accompanied by sacrificial rupture of the hydrogen bonds (circles) and large extension of the hidden coiled PNIPAM chains. Optical d) and SEM e) images of the L-NC gel film at $\phi = 23.2$ wt% after a prestrain of 150%. Arrows denote the direction of the tensile force.

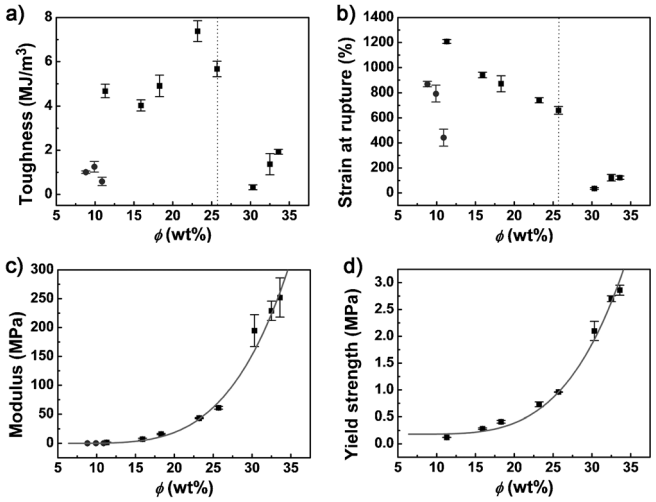

Figure 2. Effects of the clay concentration, ϕ, on the mechanical properties of R-NC (circles) and L-NC (squares) gels. a) Dependence of the toughness on the clay concentration. The toughness of the L-NC gel containing 23.2 wt% clay is six times greater than that of R-NC gels containing 9.9 wt% clay. b) Dependence of the strain at rupture on the clay concentration. For $\phi > 25.7$ wt%, the L-NC gels dramatically become brittlelike with lower extensibility and toughness. c) The initial elastic modulus, E, increases with increasing ϕ. d) The yield strength, σ_y, increases with increasing ϕ. The prediction of a typical power-law scaling of gel systems is in excellent agreement with the experimental values. The error bars correspond to the standard deviation obtained from at least three samples.

with a previous report.[17a] Moreover, a polymer chain may interact with a clay surface at multiple points.[18] The intercrosslinked polymer chains adopt a randomly coiled conformation. After the interfaces start to yield, the polymer and clay phases extensively slide against each other. The hydrogen bonds rupture and reveal significant hidden lengths of highly coiled macromolecules (Figure 1c). As a result, the process with large deformation is accompanied by dissipation of a large amount of energy.

To clarify the structure change in the tensile process, we observed the characteristic fracture morphology of L-NC gels by SEM and optical microscopy. In the linear elastic region, the film is smooth and transparent, and there is no characteristic surface structure at the optical microscope scale. After yield, an anisotropic, striplike damage pattern occurred (Figure 1d), and the transparency of the film decreased. The corresponding SEM image indicates the existence of uniform multiple cracks (Figure 1e). With a further increase of strain, the strips further fracture into smaller strips (Figure S7 in the Supporting Information) and the transparency was regained. Finally, the materials undergoing large elongation fail under platelet pull-out mode, leading to a tortuous fracture path (Figure S7 in the Supporting Information). These results indicate that the L-NC gels possess excellent damage-tolerant properties during the crack propagation. As a result, the L-NC gels synergistically combine the stiffness of inorganic clay with the dissipative ability of PNIPAM and show excellent mechanical properties.

However, the slope in the hardening region and the fracture strength decrease for the L-NC gel at $\phi_w = 25.7$ wt%. A further increase of the clay content leads to a dramatic change of the mechanical behavior. Under loading, the stress rapidly increased to the maximum and then decreased unstably without a hardening region until the sample failed. As a result, the gels became brittlelike with low fracture strain, a high elastic modulus and strength (Figure 2).

The abrupt ductile-to-brittle change of the L-NC gels ($\phi >$ 25.7 wt%) is probably attributable to the lack of hydration of the PNIPAM–clay network. Owing to the decrease of the water content, the interactions of the PNIPAM chains increase and their flexibility is lost. As a result, the L-NC gels rapidly change to stiff, strong, and solidlike brittle materials. The critical water content, defined as the onset of the brittle fracture, is about 62 wt%. A similar effect of the water content on the mechanical behavior also exists in double-network gels by drying,[19] R-NC gels by deswelling,[20] and many biological hard tissues such as nacre,[10] dentin,[21] and bone,[22] and biological soft tissues.[23]

Generally, an attractive particle system is often transformed into a jammed solid network as the volume fraction of particles exceeds a critical value. A sufficiently large stress will lead to the yield of the jammed structure. The dependence of the elastic modulus and yield strength on the particle content follows a power-law scaling.[24] As shown in Figure 2c, the dependence of the initial elastic modulus, E of L-NC gels on the clay content follows a power-law scaling [Eq. (1)],

$$E = A(\phi_v - \phi_{cv})^p \quad (1)$$

where ϕ_v is the volume fraction of clay, ϕ_{cv} is the critical volume fraction and p and A are model parameters. Here, the critical volume fraction at which the average particle spacing is equal to the particle diameter can be approximated by dividing the random-close-packed hard-sphere percolation volume fraction (around 0.64) by the aspect ratio of the clay.[25] The diameter of the clay platelets was about 28.4 nm measured by dynamic light scattering (DLS; Figure S8 in the Supporting Information) and the thickness is about 1.11 nm measured by AFM (Figure S9 in the Supporting Information). Thus the critical volume fraction, ϕ_{cv}, is calculated to be about 2.5 vol%. The experimental modulus starts to increase dramatically at $\phi_v = 2.53$ vol% for PNIPAM–clay hydrogels, because of the formation of a rigid structure.[8a] Hence, a ϕ_{cv} value of 2.5 vol% was used for the model. The predicted values of E using Equation (1) with $A = 33$ KPa and $p = 3.2$ are in excellent agreement with the experimental data.

Similarly, the increase in σ_y with increasing concentration of clay can also be modeled well by power-law scaling [Eq. (2) and Figure 2d],

$$\sigma_y = \sigma_0 + B(\phi_v - \phi_{cv})^p \quad (2)$$

where again ϕ_{cv} is 2.5 vol%. Equation (2) is used with $\{\sigma_0, B, p\} = \{150$ kPa, 1.5 kPa, 2.8 (2.8 is a model parameter and has no unit.)$\}$.

Comparison of the mechanical properties of L-NC gels, R-NC gels, SR gels, tetra-PEG gels, DN gels, and some natural hydrogels is shown in Figure 3. Because of the improved network homogeneity, SR gels, R-NC gels, and tetra-PEG

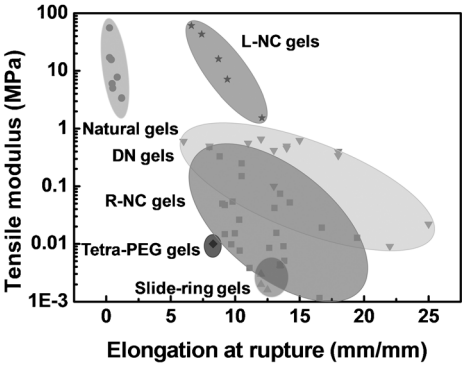

Figure 3. The tensile modulus is plotted versus the elongation at rupture for the L-NC gels and compared to four novel hydrogels developed recently and to natural hydrogels. The L-NC gels simultaneously show a striking elastic modulus, much stiffer than that of other synthetic gels, and an excellent extensibility, much higher than that of natural gels.

gels show much higher resistance to elongation (>8 times the origin length) than the first-generation hydrogels, chemically crosslinked hydrogels (extensibility of just a few percent). However, the ability of these synthetic hydrogels to undergo large deformation is often achieved at the expense of stiffness. Because of the synergistic combination of the stiffness of the first network and the dissipative ability of the second network, DN gels possess an elastic modulus of sub-MPa, a tensile strength of MPa, and large extensibility. However, the elastic modulus is still one order of magnitude lower than that of soft biological tissues. It should be noted that our L-NC gels ($\phi < 25.7$ wt %) are capable of large deformations (740–1200 %) and have the ability to generate the striking Young's modulus of 1.54–43.2 MPa, which are the highest values so far ever reported for polymeric hydrogels and are comparable to natural hydrogels (Table S1 in the Supporting Information), such as biological cartilage,[26] cornea,[27] and the strips of kelp.[28] The tensile strength is roughly comparable to double-network gels.[29] The elastic modulus, strength, and toughness for our L-NC gel samples at equilibrium are all higher than the reported values for as-prepared R-NC gels.[8,13]

In summary, we have successfully fabricated layered nanocomposite hydrogels with unique polymer/clay network structures by combination of simple vacuum-filtration self-assembly and in situ free-radical polymerization. The layered nanocomposite hydrogel possesses a nacrelike brick-and-mortar arrangement of organic and inorganic layers and shows strong mechanical properties and transparency. A lack of hydration of the PNIPAM–clay network leads to ductile-to-brittle transitions for L-NC gels. These findings provide a new concept for the design and preparation of high-performance wet-chemical materials for applications, such as tissue-engineering, sensors, artificial muscles, robust underwater anti-fouling materials, and environmentally friendly materials.

Experimental Section

Materials: A NIPAM monomer and inorganic clay (Laponite XLG, $[Mg_{5.34}Li_{0.66}Si_8O_{20}(OH)_4]Na_{0.66}$ with a layer size of 28.4 nm in diameter and 1.11 nm in thickness, Rockwood Ltd., UK) were used as received. 2,2′-Diethoxyacetophenone (DEOP) was used as initiator.

Preparation of the L-NC gel films: A dispersion of clay in ultrapure water (0.6 wt %) was stirred vigorously for 3 h. The NIPAM monomer (0.4 g) was added to a 0.6 wt % clay dispersion (15 g) and stirred for 1 h. To the transparent solution was added DEOP (40 mg) and the solution was stirred for 30 min to dissolve the initiator. Next, the mixture was filtrated under vacuum on a cellulose acetate filter membrane. The clay content was controlled through slow evaporation of water at room temperature and different filtration times. After photo-initiated free-radical polymerization ($\lambda = 365$ nm) for 25 min in nitrogen gas atmosphere, the obtained as-prepared gels were immersed in water until the equilibrium state was approached. The equilibrated hydrogels were identified as being L-NC*n* gels where *n* is the mass fraction of clay against the equilibrated gels.

Preparation of R-NC gel films: The clay, NIPAM, initiator, and water were mixed by stirring to form a transparent paste. The mass ratio of clay, NIPAM, and initiator was 67:33:3.3. The clay content was modulated by changing the amount of added water. Then, the same conditions as for the L-NC gels were applied for polymerization. The hydrogels at the equilibrium swelling state were identified as being R-NC*n* gels where *n* is also the mass fraction of clay in the equilibrated gels.

Measurements: The SEM images were obtained with a field-emission scanning electron microscope (S-4800, Hitachi) at an acceleration voltage of 3 kV. TEM images were obtained using a JEOL JEM-2100 instrument at 200 kV. X-ray diffraction (XRD) profiles were performed with $Cu_{K\alpha}$ X-rays ($\lambda = 1.54$ nm) in a step of 0.02°. The compositions of the swollen equilibrated gels were analyzed by combining mass measurements and thermal gravimetric analysis (TGA). The average diameter of a clay platelet was obtained with a dynamic light scattering (DLS) instrument (Dynapro Nano-Star, Wyatt) at 25 °C at a scattering angle of 90°. The cumulants analysis method was employed to generate size information from autocorrelation function data. AFM images were obtained by veeco bioscope catalyst atomic force microscope. The mechanical properties of the freestanding hydrogel films were measured in the tensile mode in a universal mechanical testing machine from Instron 3365, USA. The tested rectangular strips of 30–35 mm length and 5 mm width were cut out from swollen equilibrated freestanding films with a razor blade. The distance between the clamps was 10 mm and the load speed was 5 mm min^{-1}. Water mist was sprayed on the sample to avoid water loss when testing. The results for each material are based on 3–5 specimens.

Received: January 11, 2012
Published online: March 6, 2012

Keywords: clays · hydrogels · nanocomposites · polymers · self-assembly

[1] a) P. Calvert, *Adv. Mater.* **2009**, *21*, 743; b) Y. Tanaka, J. P. Gong, Y. Osada, *Prog. Polym. Sci.* **2005**, *30*, 1; c) J. A. Johnson, N. J. Turro, J. T. Koberstein, J. E. Mark, *Prog. Polym. Sci.* **2010**, *35*, 332.

[2] a) Y. Okumura, K. Ito, *Adv. Mater.* **2001**, *13*, 485; b) K. Ito, *Curr. Opin. Solid State Mater. Sci.* **2010**, *14*, 28.

[3] a) K. Haraguchi, T. Takehisa, *Adv. Mater.* **2002**, *14*, 1120; b) K. Haraguchi, *Curr. Opin. Solid State Mater. Sci.* **2007**, *11*, 47; c) Q. Wang, J. L. Mynar, M. Yoshida, E. Lee, M. Lee, K. Okuro, K. Kinbara, T. Aida, *Nature* **2010**, *463*, 339; d) M. K. Shin, G. M. Spinks, S. R. Shin, S. I. Kim, S. J. Kim, *Adv. Mater.* **2009**, *21*, 1712;

e) R. Fuhrer, E. K. Athanassiou, N. A. Luechinger, W. J. Stark, *Small* **2009**, *5*, 383.
[4] a) J. P. Gong, Y. Katsuyama, T. Kurokawa, Y. Osada, *Adv. Mater.* **2003**, *15*, 1155; b) W. Yang, H. Furukawa, J. P. Gong, *Adv. Mater.* **2008**, *20*, 4499; c) J. P. Gong, *Soft Matter* **2010**, *6*, 2583.
[5] T. Huang, H. Xu, K. Jiao, L. Zhu, H. R. Brown, H. Wang, *Adv. Mater.* **2007**, *19*, 1622.
[6] a) T. Sakai, T. Matsunaga, Y. Yamamoto, C. Ito, R. Yoshida, S. Suzuki, N. Sasaki, M. Shibayama, U.-i. Chung, *Macromolecules* **2008**, *41*, 5379; b) Y. Akagi, T. Matsunaga, M. Shibayama, U.-i. Chung, T. Sakai, *Macromolecules* **2010**, *43*, 488; c) Y. Akagi, T. Katashima, Y. Katsumoto, K. Fujii, T. Matsunaga, U.-i. Chung, M. Shibayama, T. Sakai, *Macromolecules* **2011**, *44*, 5817.
[7] K. Haraguchi, *Colloid Polym. Sci.* **2011**, *289*, 455.
[8] a) K. Haraguchi, H. J. Li, *Macromolecules* **2006**, *39*, 1898; b) Y. Liu, M. F. Zhu, X. L. Liu, W. Zhang, B. Sun, Y. M. Chen, H. J. P. Adler, *Polymer* **2006**, *47*, 1.
[9] a) B. L. Smith, T. E. Schaffer, M. Viani, J. B. Thompson, N. A. Frederick, J. Kindt, A. Belcher, G. D. Stucky, D. E. Morse, P. K. Hansma, *Nature* **1999**, *399*, 761; b) J. D. Currey, *Proc. R. Soc. London Ser. B* **1977**, *196*, 443; c) M. Sarikaya, *Microsc. Res. Tech.* **1994**, *27*, 360.
[10] A. P. Jackson, J. F. V. Vincent, R. M. Turner, *Proc. R. Soc. London Ser. B* **1988**, *234*, 415.
[11] a) S. Deville, E. Saiz, R. K. Nalla, A. P. Tomsia, *Science* **2006**, *311*, 515; b) E. Munch, M. E. Launey, D. H. Alsem, E. Saiz, A. P. Tomsia, R. O. Ritchie, *Science* **2008**, *322*, 1516; c) Z. Y. Tang, N. A. Kotov, S. Magonov, B. Ozturk, *Nat. Mater.* **2003**, *2*, 413; d) P. Podsiadlo, A. K. Kaushik, E. M. Arruda, A. M. Waas, B. S. Shim, J. Xu, H. Nandivada, B. G. Pumplin, J. Lahann, A. Ramamoorthy, N. A. Kotov, *Science* **2007**, *318*, 80; e) H.-B. Yao, Z.-H. Tan, H.-Y. Fang, S.-H. Yu, *Angew. Chem.* **2010**, *122*, 10325; *Angew. Chem. Int. Ed.* **2010**, *49*, 10127; f) L. J. Bonderer, A. R. Studart, L. J. Gauckler, *Science* **2008**, *319*, 1069; g) A. Walther, I. Bjurhager, J.-M. Malho, J. Ruokolainen, L. Berglund, O. Ikkala, *Angew. Chem.* **2010**, *122*, 6593; *Angew. Chem. Int. Ed.* **2010**, *49*, 6448; h) H.-B. Yao, H.-Y. Fang, Z.-H. Tan, L.-H. Wu, S.-H. Yu, *Angew. Chem.* **2010**, *122*, 2186; *Angew. Chem. Int. Ed.* **2010**, *49*, 2140.
[12] A. Walther, I. Bjurhager, J.-M. Malho, J. Pere, J. Ruokolainen, L. A. Berglund, O. Ikkala, *Nano Lett.* **2010**, *10*, 2742.
[13] K. Haraguchi, H. J. Li, *Angew. Chem.* **2005**, *117*, 6658; *Angew. Chem. Int. Ed.* **2005**, *44*, 6500.
[14] V. Vertlib, M. Dietiker, M. Ploetze, L. Yezek, R. Spolenak, A. M. Puzrin, *J. Mater. Res.* **2008**, *23*, 1026.
[15] a) D. A. Dikin, S. Stankovich, E. J. Zimney, R. D. Piner, G. H. B. Dommett, G. Evmenenko, S. T. Nguyen, R. S. Ruoff, *Nature* **2007**, *448*, 457; b) X. Wang, H. Bai, Z. Yao, A. Liu, G. Shi, *J. Mater. Chem.* **2010**, *20*, 9032.
[16] K. Haraguchi, T. Takada, *Macromolecules* **2010**, *43*, 4294.
[17] a) K. Haraguchi, H. J. Li, K. Matsuda, T. Takehisa, E. Elliott, *Macromolecules* **2005**, *38*, 3482; b) M. Shibayama, T. Karino, S. Miyazaki, S. Okabe, T. Takehisa, K. Haraguchi, *Macromolecules* **2005**, *38*, 10772.
[18] S. Miyazaki, H. Endo, T. Karino, K. Haraguchi, M. Shibayama, *Macromolecules* **2007**, *40*, 4287.
[19] H. Itagaki, T. Kurokawa, H. Furukawa, T. Nakajima, Y. Katsumoto, J. P. Gong, *Macromolecules* **2010**, *43*, 9495.
[20] K. Haraguchi, H.-J. Li, *J. Polym. Sci. Part B* **2009**, *47*, 2328.
[21] J. Kruzic, R. K. Nalla, J. H. Kinney, R. O. Ritchie, *Biomaterials* **2003**, *24*, 5209.
[22] J. Yan, A. Daga, R. Kumar, J. J. Mecholsky, *J. Biomech.* **2008**, *41*, 1929.
[23] *Orthopaedic Basic Science: Foundations of Clinical Practice*, 3rd ed. (Eds.: J. A. B. T. A. Einhorn, R. J. O'Keefe), American Academy of Orthopaedic Surgeons, Rosemont, IL, **2007**.
[24] V. Trappe, V. Prasad, L. Cipelletti, P. N. Segre, D. A. Weitz, *Nature* **2001**, *411*, 772.
[25] S. M. Liff, N. Kumar, G. H. McKinley, *Nat. Mater.* **2007**, *6*, 76.
[26] a) B.-y. Guo, D.-h. Liao, X.-y. Li, Y.-j. Zeng, Q.-h. Yang, *Clin. Biomech.* **2007**, *22*, 292; b) G. Bellucci, B. B. Seedhom, *Rheumatology* **2001**, *40*, 1337.
[27] Y. J. Zeng, J. Yang, K. Huang, Z. H. Lee, X. Y. Lee, *J. Biomech.* **2001**, *34*, 533.
[28] D. L. Harder, C. L. Hurd, T. Speck, *Am. J. Bot.* **2006**, *93*, 1426.
[29] a) T. Nakajima, H. Furukawa, J. P. Gong, E. K. Lin, W.-l. Wu, *Macromol. Symp.* **2010**, *291–292*, 122; b) S. Liang, Q. M. Yu, H. Yin, Z. L. Wu, T. Kurokawa, J. P. Gong, *Chem. Commun.* **2009**, 7518; c) Z. L. Wu, D. Sawada, T. Kurokawa, A. Kakugo, W. Yang, H. Furukawa, J. P. Gong, *Macromolecules* **2011**, *44*, 3542.

